

Heat Capacity of a Strongly-Interacting Fermi Gas

J. Kinast, A. Turlapov, and J. E. Thomas*

Physics Department, Duke University, Durham, North Carolina 27708-0305

*To whom correspondence should be addressed; E-mail: jet@phy.duke.edu.

(Submitted 10 September, 2004)

We report on the measurement of the heat capacity for an optically-trapped, strongly-interacting Fermi gas of atoms. For a precisely controlled energy input, we fit the spatial density of the cloud to a Thomas-Fermi distribution. We show that the fits define a reduced temperature $\tilde{T} = T/(T_F\sqrt{1+\beta})$, where β is the universal parameter introduced by O'Hara et al., (1). At $\tilde{T} = 0.33$, we observe a transition between two patterns of behavior: For $\tilde{T} = 0.33 - 2.15$, we find that the heat capacity closely corresponds to that of a trapped Fermi gas of noninteracting atoms with the mass scaled by $1/(1+\beta)$. At low temperatures $\tilde{T} = 0.04 - 0.33$, the heat capacity scales as \tilde{T}^α , where $\alpha = 1.53(0.15)$, corresponding to bosonic (fermion pair) excitations of a condensate.

Strongly-interacting, degenerate atomic Fermi gases (1) provide a paradigm for strong interactions in nature. Measurements of the interaction energy (1, 2, 3, 4) test predictions of universal interactions in nuclear matter (5, 6, 7, 8), as well as effective field theories of strong interac-

tions (9). The anisotropic expansion observed for strongly-interacting Fermi gases (1) is analogous to the “elliptic flow” of a quark-gluon plasma (10). High temperature superfluidity has been predicted in strongly-interacting Fermi gases (11, 12, 13), which can be used to test theories of high temperature superconductivity (14). Microscopic evidence for high temperature superfluidity has been obtained in the condensation of preformed pairs (15, 16) and in radio frequency measurements of the pairing gap (17). Macroscopic evidence arises in anisotropic expansion (1) and in collective excitations (18, 19). We report on the measurement of the heat capacity for a strongly-interacting Fermi gas of ^6Li atoms, confined in an optical trap. Our measurements examine the fundamental thermodynamics of the gas. At moderate temperatures, the total energy corresponds to that of a trapped noninteracting Fermi gas with increased mass. Low temperature measurements reveal a quite different scaling, corresponding to a gas of bosons interacting via fermions (20).

A feature common to all of these strongly interacting Fermi systems is that scattering interactions between spin-up and spin-down fermions have a zero energy scattering length a which far exceeds the interparticle spacing. In two-component atomic Fermi gases, this is achieved by magnetically tuning the diatomic interaction potentials into the vicinity of an s-wave collisional (Feshbach) resonance (21). Assuming that the potentials have a short range compared to the interparticle spacing, the gas is expected to exhibit universal features: The scattering length $|a| \rightarrow \infty$ and cannot determine the properties of the system, which then depend only on the Fermi energy, the temperature, and dimensionless universal parameters (5, 6, 7). One such parameter, β (1, 2), determines the interaction energy of the gas in units of the local Fermi energy. This parameter has now been measured by several groups (1, 2, 3, 4) and is in reasonable agreement with the best current quantum Monte Carlo calculations (8). The concept of universal thermodynamics has been greatly expanded by Ho (22), who determined the general structure of a unitary gas (23), and used it to study the temperature dependence of preformed pair con-

densation in Fermi gases (24, 25). We use arguments based on universal thermodynamics to explain the temperature dependence of the heat capacity in the region above the transition.

Heat capacity is determined in our experiments by measuring the reduced temperature \tilde{T} of the gas for a predetermined energy input. The experiments yield the total energy of the gas as a function \tilde{T} . In the following, we describe how the gas is prepared, how a precisely known energy is added to the gas, and our method of thermometry.

We prepare a degenerate 50-50 mixture of the two lowest spin states of ^6Li atoms by forced evaporation in an ultrastable CO_2 laser trap (26) as described previously (1). At a bias magnetic field of 840 G, just above the Feshbach resonance, the trap depth is lowered by a factor of $\simeq 580$ in a few seconds (1, 18) and then recompressed to 4.6% of the full trap depth in 0.5 s and held for 0.5 s to assure equilibrium. After a controlled amount of energy is added to the gas, as described below, the gas is allowed to thermalize for 0.1 s. Finally, the gas is released from the trap and imaged at 840 G to determine the number of atoms and the temperature.

The number of atoms and the reduced temperature are determined from the column density obtained by absorption imaging of the expanded cloud after 1 ms time of flight, using a two-level state-selective cycling transition (1, 18). In the measurements of the cloud column density, we take optical saturation into account exactly and arrange to have very small optical pumping out of the two-level system. For our trap, the total number of atoms is $N = 2.0(0.2) \times 10^5$. From the measured trap frequencies, corrected for anharmonicity, we obtain $\omega_{\perp} = \sqrt{\omega_x \omega_y} = 2\pi \times 1696(10)$ Hz and $\omega_z = 2\pi \times 72(5)$ Hz, so that $\bar{\omega} = (\omega_x \omega_y \omega_z)^{1/3} = 2\pi \times 592(14)$ Hz is the mean oscillation frequency. For these parameters, the typical Fermi temperature $T_F = (3N)^{1/3} \hbar \bar{\omega} / k_B$ for a noninteracting gas is $\simeq 2.4 \mu\text{K}$, small compared to the final trap depth of $U_0/k_B = 35 \mu\text{K}$. The column density is spatially integrated along the trap axial direction to yield one dimensional, transverse spatial distributions $n(x)$, which are fit using finite temperature Thomas-Fermi distributions. The reduced temperatures measured using the

Thomas-Fermi fits, $(T/T_F)_{fit}$, are in the range 0.04–2.15 for the strongly-interacting gas and 0.2–1.1 for the noninteracting gas.

Energy is precisely added to the trapped gas at fixed atom number by releasing the cloud from the trap and permitting it to expand for a short time t_{heat} after which the gas is recaptured. Even for the strongly-interacting gas, the energy input is well-defined, because the energy change arises only from the trapping potential and the gas is always initially at the same very low temperature. During the times t_{heat} used in the experiments, the axial size of the gas changes negligibly, while transverse dimensions expand by a factor $b_{\perp}(t_{heat})$. Hence, the harmonic trapping potential energy in each of the two transverse directions increases by a factor $b_{\perp}^2(t_{heat})$.

The initial potential energy is readily determined at zero temperature. This follows from the equation of state of the gas, $(1 + \beta)\epsilon_F(\mathbf{x}) + U_{trap}(\mathbf{x}) = \mu_0$ (1), where $\epsilon_F(\mathbf{x})$ is the local Fermi energy, U_{trap} is the harmonic trapping potential, and μ_0 is the global chemical potential (27). The equation of state is equivalent to that of a harmonically trapped noninteracting gas with an effective mass (7), which in our notation is $M_{eff} = M/(1 + \beta)$, where M is the bare mass. Thus, the mean potential energy is half of the total energy. Since $\beta < 0$ (8), $M_{eff} > M$, so that the effective oscillation frequencies and the chemical potential are simply scaled down, i.e., $\mu_0 = k_B T_F \sqrt{1 + \beta}$ (1, 2). The total energy at zero temperature is $E_0 = (3/4)N\mu_0$. For each direction, the initial potential energy at zero temperature is $E_0/6$. The total energy of the gas after heating then is given by (28),

$$E(t_{heat}) = \eta_i E_0 \left[\frac{2}{3} + \frac{1}{3} b_{\perp}^2(t_{heat}) \right], \quad (1)$$

where η_i is a correction factor arising from the finite temperature of the gas prior to the energy input. For the noninteracting gas, the Sommerfeld correction yields $\eta_i = 1 + 2\pi^2(T_i/T_F)_{fit}^2/3$ (29). For the strongly-interacting gas where the initial temperature is very low, we also assume a

Sommerfeld correction, and find η_i is 1.01, which hardly affects the energy scale. The strongly-interacting gas exhibits hydrodynamic, anisotropic expansion (*I*), so that $b_\perp = b_\perp^H$ is a hydrodynamic expansion factor (*I*, 30). We use a ballistic expansion factor for the noninteracting gas, $b_\perp^B(t) = \sqrt{1 + (\omega_\perp t)^2}$. In the experiments, the range of $\omega_\perp t_{heat} \simeq 0 - 5$.

Thermometry of strongly-interacting Fermi gases is not well understood. However, a useful temperature scale can be established by using a Thomas-Fermi fit to the spatial density of the cloud, as suggested by Jackson, Pedri, and Stringari (*31*). We now show that this method defines a reduced temperature scale $\tilde{T} = T/(T_F\sqrt{1+\beta})$.

Following Jackson et al., (*31*), we assume an effective Hamiltonian H of a noninteracting, harmonically trapped gas: The energy for the x-direction is taken to be $H_x = p_x^2/(2M) + M\omega_x^2 x^2/2$, and similarly for the y- and z-directions. The temperature scale follows from the spatial density, $n(\mathbf{x}) = \int d^3\mathbf{p} f(\mathbf{x}, \mathbf{p})/h^3$, where $f[(H(\mathbf{x}, \mathbf{p}) - \mu)/k_B T]$ is the occupation number. We can factor the chemical potential at zero temperature, $\mu(0)$, out of the argument of f . In this case, the argument of f takes the form $\mu(0)/(k_B T)[H/\mu(0) - \mu/\mu(0)]$. The potential energy for the x-direction yields $M\omega_x^2 x^2/[2\mu(0)] \equiv x^2/\sigma_x'^2$, where σ_x' is the zero temperature Fermi radius of the cloud in the x-direction.

In the experiments, we first determine the two parameters, σ_x' and $k_B T/\mu(0)$, from the fit to the measured transverse spatial distributions at the lowest temperature, where the shape is nearly a zero temperature Thomas-Fermi distribution, and σ_x' is nearly uncorrelated with $k_B T/\mu(0)$. Now, at zero temperature, the radius of the trapped cloud for the strongly-interacting gas takes the form $\sigma_x' = \sigma_x(1 + \beta)^{1/4}$ (*2*), where $\sigma_x = \sqrt{2k_B T_F/(M\omega_x^2)}$ is the radius for a noninteracting gas. To determine σ_x' , we measure the size of the cloud after 1 ms of expansion, and scale it down by the known hydrodynamic expansion factor of 13.3 (*I*, 30). We then determine the Fermi radius $\sigma_x' = 11.98/13.3 = 0.901(0.021) \mu\text{m} (N/2)^{1/6}$. Using $\sigma_x = 1.065 \mu\text{m} (N/2)^{1/6}$ for our trap parameters, yields $\beta = -0.49(0.04)$, in good agreement with the value $\beta = -0.56$

obtained from current quantum Monte Carlo calculations (8). Since the Fermi radius σ'_x of the gas and therefore β is determined, we then have $\mu(0) = M\omega_x^2\sigma_x'^2/2 = k_B T_F\sqrt{1+\beta}$. This is just the global chemical potential, μ_0 , as it should be.

In the fits for all higher temperatures, we vary only $k_B T/\mu_0$, and hold σ'_x (and hence β) constant. Thus, over a temperature range where $\beta \simeq \text{const}$, we have set the reduced temperature scale in the Thomas-Fermi fits to be

$$\left(\frac{T}{T_F}\right)_{fit} \equiv \frac{T}{T_F\sqrt{1+\beta}}. \quad (2)$$

We now apply our energy input and thermometry methods to determine the heat capacity of an optically trapped Fermi gas. To obtain high resolution data for the reduced temperature versus total energy, 30-40 different heating times are chosen. The data for each of these heating times are acquired in a random order to minimize systematic error. Ten complete runs are taken through the entire sequence.

To test the method with a known system, we first measure the reduced temperature as a function of input energy for a noninteracting Fermi gas at 526 G where $\beta = 0$. The gas is initially cooled to $(T/T_F)_{fit} = 0.2$ by 30 seconds of forced evaporation at 300 G as described previously (18), and then heated as described above. The top (green) data in Fig. 1, shows the results on a $\ln - \ln$ scale. The vertical axis displays the normalized energy input $E/E_0 - 1$, where the total energy E is calculated using Eq. 1, in units of the initial energy E_0 for a zero temperature gas. The horizontal axis is the reduced temperature $(T/T_F)_{fit}$ (which in this case is just T/T_F) obtained from the T-F fits to the one-dimensional transverse spatial distributions.

The upper red curve in Fig. 1 shows the energy E/E_0 predicted for an ideal, trapped Fermi gas as a function of T/T_F . The chemical potential and energy are calculated using a finite temperature Fermi distribution and the density of states for the trapped gas. To obtain very good agreement at all temperatures, we use the density of states for a gaussian potential well (26),

rather than the harmonic oscillator approximation.

Striking results are obtained for the strongly interacting gas at 840 G, lower (blue) data, Fig. 1. Here the gas is cooled to $(T/T_F)_{fit} = 0.04$ and then heated. As shown in the $\ln - \ln$ plot of Fig. 1, the data reveal a transition in slope at $(T/T_F)_{fit} \simeq 0.3$.

First we discuss the region above 0.3. Here, we find that the data are in good agreement with the reduced energy E/E_0 predicted for an ideal, trapped Fermi gas with T/T_F replaced by $(T/T_F)_{fit}$ (red curve). We now show that this behavior can be explained as a consequence of the universal thermodynamics expected for a strongly-interacting Fermi gas (I, 5, 23). We begin by determining the entropy and energy of the gas at low temperature.

We consider the consequences of assuming that the entropy at low temperature takes the same form as for a harmonically trapped ideal Fermi gas, $S = \pi^2 N k_B^2 (T/\mu_0)$, which follows from the effective mass picture (32). Hence, $S = \pi^2 N k_B (T/T_F)_{fit}$. Using $(\partial S/\partial E) = 1/T$ then yields $E/E_0 = 1 + (2\pi^2/3)(T/T_F)_{fit}^2$, where $E_0 = 3N\mu_0/4$. Hence, the energy at low temperature takes the universal form of a Sommerfeld expansion for an ideal gas, with T/T_F replaced by $(T/T_F)_{fit}$. This suggests that for any temperature, the strongly interacting Fermi gas can be described by noninteracting gas theory with T/T_F replaced by $(T/T_F)_{fit}$. These results should be valid in the temperature range where β is approximately constant and the gas is normal, so that the superfluid gap does not suppress the contribution of fermionic single particle excitations.

From Fig. 1, we find that the data in the temperature range $(T/T_F)_{fit} \geq 0.3$ is well fit by the scaled ideal Fermi gas model. Note that we cannot determine if β is changing from the high temperature slope (on a linear scale). There, our T-F distribution is a Maxwell-Boltzmann for any value of β . Hence, the measured slope of the energy versus reduced temperature will always agree with the ideal gas prediction $3Nk_B$ when the gas becomes classical.

Nonfermionic scaling of the energy with temperature is observed for $(T/T_F)_{fit} \leq 0.3$, as

shown in the $\ln - \ln$ plot of Fig. 1 and in the linear low temperature plot of Fig. 2. The data deviate from the scaled ideal Fermi gas theory (red curve). Fitting a power law $E/E_0 = 1 + b(T/T_F)_{fit}^c$ (green curve) to the low temperature data, we obtain the best fit with $b = 9.76(1.94)$ and $c = 1 + \alpha = 2.53(0.15)$. The χ^2 per degree of freedom for this fit is 1.4. Fitting a quadratic temperature dependence yields $E/E_0 = 1 + d(T/T_F)_{fit}^2$, where $d = 4.81(0.18)$, and a larger χ^2 per degree of freedom of 5.2. In addition, a T^4 power law fit yields a χ^2 per degree of freedom of 7.1, showing that the gas is not a BEC of small weakly interacting molecules.

The $T^{5/2}$ scaling for the energy corresponds to a total entropy $S \propto (T/T_F)_{fit}^{3/2}$. One can understand this result as arising from thermal excitation of low energy bosons (fermion pairs) (14). By contrast, one expects the fermionic contribution is exponentially suppressed by the superfluid gap (20). A simple picture of the $5/2$ power scaling is that short wavelength thermal excitations increase the local kinetic energy of bound pairs without breaking them, yielding the density of states and energy for free particles in three dimensions (33).

We estimate the transition temperature from the intersection point of the power law fit and the scaled ideal gas prediction. This yields $(T_c/T_F)_{fit} = 0.33(.02)$, where we include only the error bar from the fit. For $\beta = -0.49$, we then obtain $T_c/T_F = 0.24(.02)$, close to predictions for the cross over regime which have been made over the last decade (14, 34). From the power law fit, the low temperature heat capacity is $C/(Nk_B) = 31(6) (T/T_F)^{1.53(.16)}$.

Our energy input and thermometry techniques can be used to determine the increase in entropy which arises during the collisional expansion of a strongly-interacting, hydrodynamic gas, as suggested by Jackson et al., (31). Recently, we have used this method to precisely measure a transition temperature for the damping rate of the radial breathing mode, which will be discussed elsewhere.

References and Notes

1. K. M. O'Hara, S. L. Hemmer, M. E. Gehm, S. R. Granade, J. E. Thomas, *Science* **298**, 2179 (2002).
2. M. E. Gehm, S. L. Hemmer, S. R. Granade, K. M. O'Hara, J. E. Thomas, *Phys. Rev. A* **68**, 011401(R) (2003).
3. T. Bourdel, *et al.*, *Phys. Rev. Lett.* **93**, 050401 (2004).
4. M. Bartenstein, *et al.*, *Phys. Rev. Lett.* **92**, 120401 (2004).
5. H. Heiselberg, *Phys. Rev. A* **63**, 043606 (2001).
6. G. F. Bertsch proposed the problem of determining the ground state of a two-component Fermi gas with a long scattering length, <http://www.phys.washington.edu/mbx/george.html>.
7. J. G. A. Baker, *Phys. Rev. C* **60**, 054311 (1999).
8. J. Carlson, S.-Y. Chang, V. R. Pandharipande, K. E. Schmidt, *Phys. Rev. Lett.* **91**, 050401 (2003).
9. J. V. Steele, Effective field theory power counting at finite density (2000). nucl-th/0010066.
10. P. F. Kolb, U. Heinz, *Quark Gluon Plasma 3* (World Scientific, 2003). See Hydrodynamic Description of Ultrarelativistic Heavy Ion Collisions, arXiv: nucl-th/0305084.
11. M. Holland, S. J. J. M. F. Kokkelmans, M. L. Chiofalo, R. Walser, *Phys. Rev. Lett.* **87**, 120406 (2001).
12. E. Timmermans, K. Furuya, P. W. Milonni, A. K. Kerman, *Phys. Lett. A* **285**, 228 (2001).

13. Y. Ohashi, A. Griffin, *Phys. Rev. Lett.* **89**, 130402 (2002).
14. Q. Chen, J. Stajic, S. Tan, K. Levin, BCS-BEC crossover: From high temperature superconductors to ultracold superfluids (2004). ArXiv:cond-mat/0404274.
15. C. A. Regal, M. Greiner, D. S. Jin, *Phys. Rev. Lett.* **92**, 040403 (2004).
16. M. W. Zwierlein, C. A. Stan, C. H. Schunck, A. J. K. S. M. F. Raupach, W. Ketterle, *Phys. Rev. Lett.* **92**, 120403 (2004).
17. C. Chin, *et al.*, *Science* **305**, 1128 (2004).
18. J. Kinast, S. L. Hemmer, M. E. Gehm, A. Turlapov, J. E. Thomas, *Phys. Rev. Lett.* **92**, 150402 (2004).
19. M. Bartenstein, *et al.*, *Phys. Rev. Lett.* **92**, 203201 (2004).
20. We thank K. Levin for suggesting this explanation to us, K. Levin, private communication.
21. M. Houbiers, H. T. C. Stoof, W. I. McAlexander, R. G. Hulet, *Phys. Rev. A* **57**, R1497 (1998).
22. T.-L. Ho, E. Mueller, *Phys. Rev. Lett.* **92**, 160404 (2004).
23. T.-L. Ho, *Phys. Rev. Lett.* **92**, 090402 (2004).
24. R. B. Diener, T.-L. Ho, Projecting fermion pair condensates into molecular condensates (2004). ArXiv:cond-mat/0404517.
25. R. B. Diener, T.-L. Ho, The conditions for universality at resonance and direct measurement of pair wavefunctions using rf spectroscopy (2004). ArXiv:cond-mat/04045174.
26. K. M. O'Hara, *et al.*, *Phys. Rev. Lett.* **82**, 4204 (1999).

27. This equation of state is supported by both the measured anisotropic expansion (*I*) and the measured radial breathing mode frequency at 840 G near resonance (35), which is in excellent agreement with predictions (36, 37) for a unitary, hydrodynamic Fermi gas.
28. We include an anharmonic correction arising from the gaussian trapping potential. For a cylindrically symmetric trap, $\Delta E/E_0 = -\mu_0[2b_{\perp}^4(t) + b_{\perp}^2(t) - 3]/(30U_0) + \mu_0^2[4b_{\perp}^6(t) + 2b_{\perp}^4(t) + 3b_{\perp}^2(t) - 9]/(360U_0^2)$. Note that we do not assume cylindrical symmetry in determining the energy input for our experiments.
29. N. W. Ashcroft, N. D. Mermin, *Solid State Physics* (Holt, Rinehart, and Winston, Philadelphia, 1976).
30. C. Menotti, P. Pedri, S. Stringari, *Phys. Rev. Lett.* **89**, 250402 (2002).
31. B. Jackson, P. Pedri, S. Stringari, Collisions and expansion of an ultracold dilute fermi gas (2004). ArXiv:cond-mat/0404175.
32. Note that to leading order, the total entropy is linear in the temperature, so that the integral over energy can be replaced by its zero temperature approximation.
33. This picture was suggested to us by J. Ho, private communication.
34. C. A. R. S. de Melo, M. Randeria, J. R. Engelbrecht, *Phys. Rev. Lett.* **71**, 3202 (1993).
35. J. Kinast, A. Turlapov, J. E. Thomas, Breakdown of hydrodynamics in the radial breathing mode of a strongly-interacting fermi gas (2004). ArXiv:cond-mat/0408634.
36. S. Stringari, *Europhys. Lett.* **65**, 749 (2004).
37. H. Heiselberg, *Phys. Rev. Lett.* **93**, 040402 (2004).

38. This research is supported by the Chemical Sciences, Geosciences and Biosciences Division of the Office of Basic Energy Sciences, Office of Science, U. S. Department of Energy, the Physics Divisions of the Army Research Office and the National Science Foundation, and the Fundamental Physics in Microgravity Research program of the National Aeronautics and Space Administration.

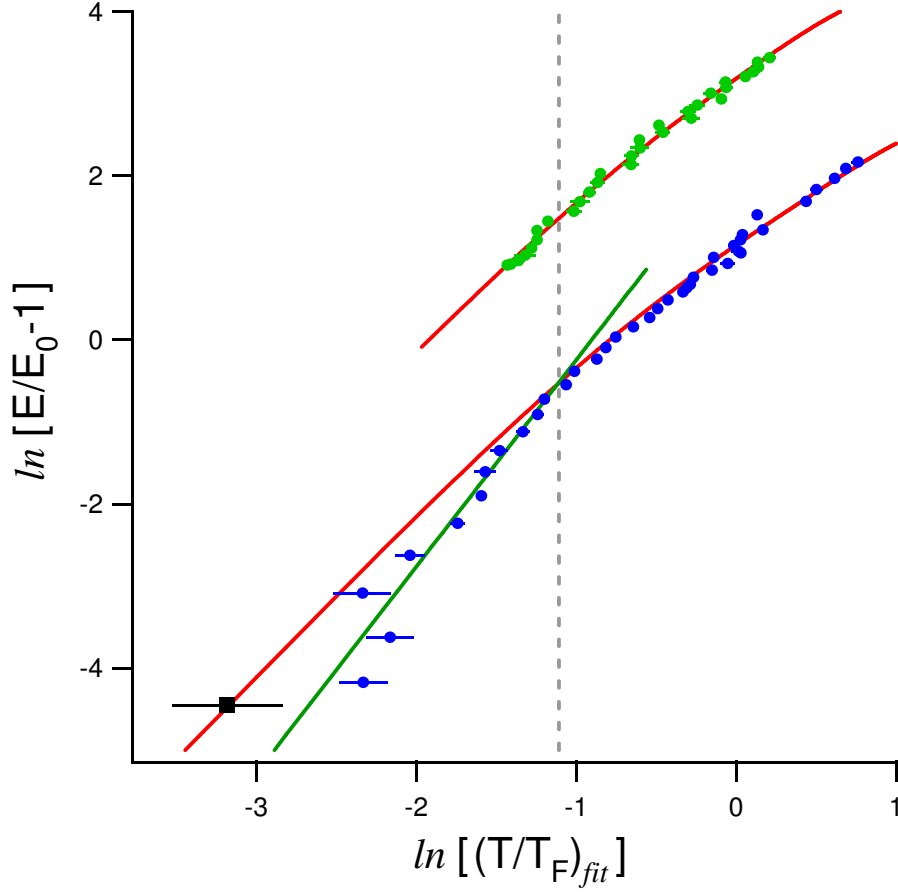


Figure 1: Energy input versus reduced temperature $(T/T_F)_{fit}$ on a $\ln - \ln$ scale. Green circles: noninteracting Fermi gas data (shifted vertically by 2 for clarity); Blue circles: strongly interacting Fermi gas data; Red lines: Predicted energy, E/E_0 , for an ideal, trapped Fermi gas as a function of reduced temperature $(T/T_F)_{fit}$; Green line: best fit power law $9.76(T/T_F)_{fit}^{2.53}$. Dotted line indicates transition temperature, $(T/T_F)_{fit} = 0.33$. Note the lowest temperature point (black square) is not included in the fits, as it is constrained to lie on the red curve.

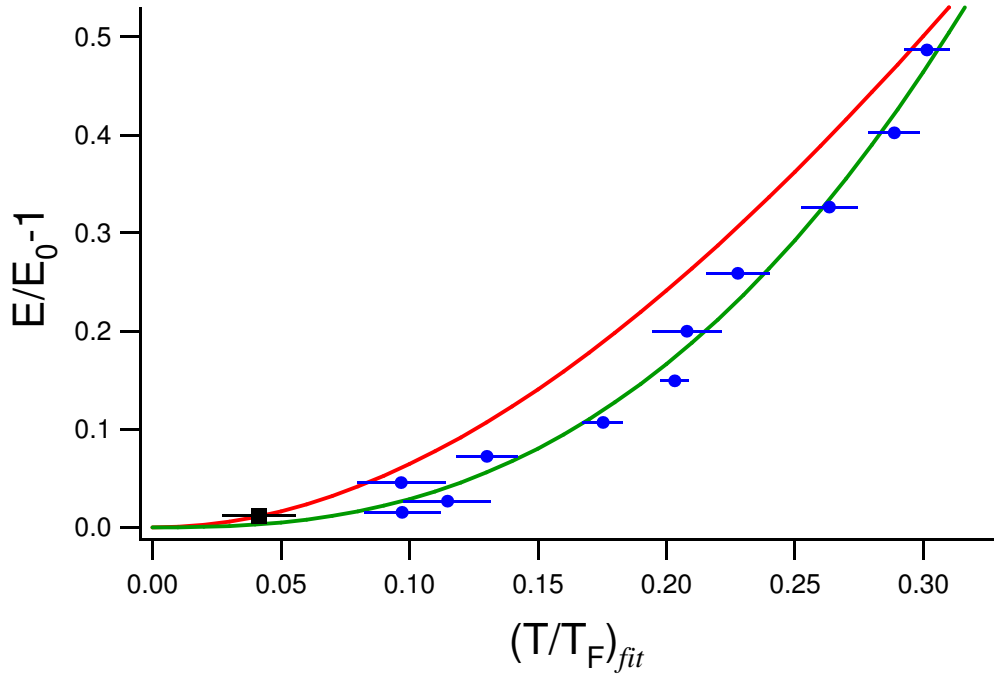


Figure 2: Strongly-interacting Fermi gas below the transition temperature. E/E_0 versus $(T/T_F)_{fit}$ on a linear scale. Green line, best fit power law $9.76 (T/T_F)_{fit}^{2.53}$. Red line: Predicted E/E_0 for an ideal Fermi gas as a function of $(T/T_F)_{fit}$. Note the lowest temperature point (black square) is not included in the fits, as it is constrained to lie on the red curve.